Chin. Geogra. Sci. 2016 Vol. 26 No. 4 pp. 439–455
doi: 10.1007/s11769-016-0818-x

Springer Science Press
www.springerlink.com/content/1002-0063

Evaluation of Latest TMPA and CMORPH Precipitation Products with Independent Rain Gauge Observation Networks over High-latitude and Low-latitude Basins in China

JIANG Shanhu[1], REN Liliang[1], YONG Bin[1], HONG Yang[2], YANG Xiaoli[1], YUAN Fei[1]

(1. *State Key Laboratory of Hydrology-Water Resources and Hydraulic Engineering*, *Hohai University*, *Nanjing* 210098, *China*; 2. *School of Civil Engineering and Environmental Sciences*, *School of Meteorology*, *University of Oklahoma*, *Oklahoma* 73019, *USA*)

Abstract: The Tropical Rainfall Measuring Mission (TRMM) Multi-satellite Precipitation Analysis (TMPA) and National Oceanic and Atmospheric Administration (NOAA) Climate Prediction Center (CPC) morphing technique (CMORPH) are two important multi-satellite precipitation products in TRMM-era and perform important functions in GPM-era. Both TMPA and CMORPH systems simultaneously upgraded their retrieval algorithms and released their latest version of precipitation data in 2013. In this study, the latest TMPA and CMORPH products (i.e., Version-7 real-time TMPA (T-rt) and gauge-adjusted TMPA (T-adj), and Version-1.0 real-time CMORPH (C-rt) and Version-1.0 gauge-adjusted CMORPH (C-adj)) are evaluated and intercompared by using independent rain gauge observations for a 12-year (2000–2011) period over two typical basins in China with different geographical and climate conditions. Results indicate that all TMPA and CMORPH products tend to overestimate precipitation for the high-latitude semiarid Laoha River Basin and underestimate it for the low-latitude humid Mishui Basin. Overall, the satellite precipitation products exhibit superior performance over Mishui Basin than that over Laoha River Basin. The C-adj presents the best performance over the high-latitude Laoha River Basin, whereas T-adj showed the best performance over the low-latitude Mishui Basin. The two gauge-adjusted products demonstrate potential in water resource management. However, the accuracy of two real-time satellite precipitation products demonstrates large variability in the two validation basins. The C-rt reaches a similar accuracy level with the gauge-adjusted satellite precipitation products in the high-latitude Laoha River Basin, and T-rt performs well in the low-latitude Mishui Basin. The study also reveals that all satellite precipitation products obviously overestimate light rain amounts and events over Laoha River Basin, whereas they underestimate the amount and events over Mishui Basin. The findings of the precision characteristics associated with the latest TMPA and CMORPH precipitation products at different basins will offer satellite precipitation users an enhanced understanding of the applicability of the latest TMPA and CMORPH for water resource management, hydrologic process simulation, and hydrometeorological disaster prediction in other similar regions in China. The findings will also be useful for IMERG algorithm development and update in GPM-era.

Keywords: satellite precipitation; Tropical Rainfall Measuring Mission (TRMM) Multi-satellite Precipitation Analysis (TMPA); Climate Prediction Center morphing technique (CMORPH); precision evaluation

Citation: Jiang Shanhu, Ren Liliang, Yong Bin, Hong Yang, Yang Xiaoli, Yuan Fei, 2016. Evaluation of latest TMPA and CMORPH precipitation products with independent rain gauge observation networks over high-latitude and low-latitude basins in China. *Chinese Geographical Science*, 26(4): 439–455. doi: 10.1007/s11769-016-0818-x

1 Introduction

Precipitation is a fundamental hydrometeorological element of the climate system and the terrestrial hydrologic cycle system, and temporal and spatial variations of precipitation affect land surface hydrological fluxes and

Received date: 2015-06-18; accepted date: 2015-09-23

Foundation item: Under the auspices of Programme of Introducing Talents of Discipline to Universities by Ministry of Education and the State Administration of Foreign Experts Affairs, China (the 111 Project, No. B08048), National Natural Science Foundation of China (No. 41501017), Natural Science Foundation of Jiangsu Province (No. BK20150815)

Corresponding author: REN Liliang. E-mail: njRLL9999@126.com

states significantly (Su *et al*., 2008; Kidd and Huffman, 2011; Kucera *et al*., 2013; Hou *et al*., 2014). Thus, obtaining accurate and reliable precipitation information is crucial for regional and global water resource management, climate change research, hydrologic process simulation, and drought/flood disaster prediction (Hong *et al*., 2007; Jiang *et al*., 2012; Wu *et al*., 2014). Precipitation data are traditionally acquired from ground-based observations (using rain gauges and/or ground-based weather radars). During recent years, the growing availability of high-resolution satellite precipitation products has provided an unprecedented opportunity for hydrologists and meteorologists to use satellite-retrieved precipitation data in hydrometeorological applications over medium to large river watersheds, especially for data-scarce or ungauged basins (Jiang *et al*., 2010; 2014). On February 27, 2014, the Global Precipitation Measurement (GPM; http://pmm.nasa.gov/GPM) core observatory was launched. The GPM mission will provide users with accurate and higher spatial and temporal resolution global precipitation products named Integrated Multi-satellite Retrievals for GPM (IMERG; 0.1°, 0.5 h). Satellite precipitation retrieval will transform from the Tropical Rainfall Measuring Mission (TRMM)-era to GPM-era. Meanwhile, as the prelude of GPM, current operational TRMM Multi-satellite Precipitation Analysis products (TMPA) and the National Oceanic and Atmospheric Administration (NOAA) Climate Prediction Center (CPC) morphing technique (CMORPH) still have an important function in multi-satellite precipitation observations (Joyce *et al*., 2004; Huffman *et al*., 2007). These two satellite precipitation products have experienced significant success and have been widely scrutinized by hydrologists and meteorologists in the past decade (Behrangi *et al*., 2011; Bitew and Gebremichael, 2011). In addition, both TMPA and CMORPH systems have upgraded their retrieval algorithms and released their latest version precipitation products almost simultaneously before the GPM mission was implemented.

The TMPA, which combines low-Earth orbiting microwave (MW) data and geostationary infrared (IR) data from all available precipitation-related satellite platforms, aims to produce the best estimates of quasi-global (50°N–50°S) precipitation at the TRMM-era (Huffman *et al*., 2007; Yong *et al*., 2014). Since its development, the TMPA algorithm has undergone several upgrades because of the use of new sensors and the upgrade of algorithms (Yong *et al*., 2012). The latest upgrade occurred on January 28, 2013. On this date, Version 7 of the TMPA satellite precipitation products was released, and the related algorithm was adopted as the initial algorithm for the GPM mission. Four main upgrades of the TMPA Version 7 were conducted relative to the original Version 6: 1) the Special Sensor Microwave Imager Sounder (SSMIS) on Defense Meteorological Satellite Program (DSMP) F-16 satellites were incorporated into TMPA real-time Version and were anticipated to further improve the data accuracy of microwave precipitation estimates; 2) the inhomogeneously processed Advanced Microwave Sounding Unit (AMSU) record in Version 6 is uniformly processed in Version 7; 3) TMPA Version 7 uses the new Global Precipitation Climatology Centre (GPCC) full gauge analysis whenever the GPCC monitoring gauge analysis is available from 2010; 4) the TRMM Microwave Imager (TMI) and Special Sensor Microwave Imager (SSM/I) input data were upgraded to the Goddard Profiling Algorithm (GPROF) 2010 algorithm (Huffman and Bolvin, 2013). The CMORPH technique uses the directness of low-Earth orbiting MW observations with cloud motion derived from geostationary IR data to estimate precipitation. Moreover, the technique is flexible and allows precipitation estimates from any MW satellite source to be incorporated (Joyce *et al*., 2004). At the NOAA CPC, CMORPH was reprocessed with a fixed algorithm by using inputs of the same versions as that in 2014. The reprocessed CMORPH is called Version 1.0, and the original CMORPH is called Version 0.x. Two main differences of the CMORPH Version 1.0 relative to the original Version 0.x are as follows: 1) Version 1.0 covers the entire TRMM/GPM-era from Jan. 1998 to the present, whereas Version 0.x started from Dec. 2002; 2) Version 1.0 includes raw, satellite-only precipitation estimates, as well as bias-corrected and gauge satellite-blended precipitation products, whereas Version 0.x presents only satellite-only products (Xie, 2013).

Previous studies focused on evaluating the performance of high-resolution multi-satellite precipitation products over different climatic regions in China, and TMPA and CMORPH are found to be the best performing satellite precipitation estimates in China at the TRMM-era, with obvious variability dependence on geography and climate conditions (Shen *et al*., 2010; Li

et al., 2013; Hu *et al*., 2014; Li *et al*., 2014; Liu *et al*., 2014; Shen *et al*., 2014; Tong *et al*., 2014). Shen *et al*. (2010) investigated the performance of six popular satellite precipitation products over mainland China and found that gauge adjustment procedures applied in the gauge-adjusted TMPA product (Version 6) removed the large-scale regional and seasonal bias that existed in real-time pure satellite observations. They also found that CMORPH performed best in depicting the spatial pattern and temporal variations of precipitation. Moreover, on the basis of the accuracy analysis of high-resolution satellite precipitation products over mainland China, Shen *et al*. (2014) developed a high spatiotemporal gauge-satellite merged precipitation analysis over China by merging rain gauge data and CMORPH precipitation data. Hu *et al*. (2014) evaluated six high-resolution satellite precipitation estimates at multi-scale over a humid region in China. The group found that TMPA and CMORPH exhibited superior performance. With the latest updates of TMPA and CMORPH inversion algorithms, the error characteristics of TMPA Version 7 and CMORPH Version 1.0 reveal several changes in China. For example, Chen *et al*. (2013) analyzed the similarity and difference of the TMPA Version 6 and Version 7 precipitation products over China, and found that the gauge-adjusted TMPA Version 7 product clearly improves upon Version 6 over China. However, the performance of CMORPH Version 1.0 products in comparison with TMAP version 7 over river basins in China remains unknown. The characteristics of the latest TMPA and CMORPH precipitation products over different watersheds in China should be investigated by validation with in situ precipitation measurements. This validation will be relevant and useful for the application and update of IMERG in the GPM-era. Thus, this study aims to intercompare TMPA Version 7 and CMORPH Version 1.0 precipitation products (i.e., Version-7 real-time TMPA (T-rt) and gauge-adjusted TMPA (T-adj), and Version-1.0 real-time CMORPH (C-rt) and Version-1.0 gauge-adjusted CMORPH (C-adj)) with dense rain gauge observations over two typical high- and low-latitude basins in China. We will focus on: 1) the spatial-temporal error characteristics of the four latest satellite precipitation products, including two real-time versions of T-rt and C-rt and two gauge-adjusted versions of T-adj and C-adj, and whether the CMORPH show good performance in a high-latitude river basin; 2) the differences and similarities of four satellite precipitation products in high-latitude Laoha River Basin and low-latitude Mishui Basin; and 3) methods of achieving the best hydrometeorological application using the respective advantages of the four satellite precipitation products.

2 Materials and Methods

2.1 Study area

The two basins selected in this study are the high- latitude Laoha River Basin, which is located beyond the TRMM TMI/precipitation radar (PR) nominal coverage (38°N–38°S) in northern China, and the low-latitude Mishui Basin, which is situated within the TRMM nominal coverage in southern China (Fig. 1). The Laoha River Basin, which has a drainage area of 18 112 km^2 and 52 rain gauges, lies upstream of the West Liaohe River Basin (41°00′–42°45′N, 117°15′–120°00′E). Elevation within the basin ranges from 427 m to 2054 m, and topography descends significantly from southwest to northeast. The area is dominated by a temperate semiarid continental monsoon climate, and the average annual temperature and precipitation are approximately 7.5℃ and 424 mm, respectively. The spatial and temporal distribution of precipitation within the Laoha River Basin is uneven, and approximately 80% of the annual precipitation occurs between May and September. The Mishui Basin (26°00′–27°12′N, 112°51′–114°12′E), located southeast of Hunan Province in South China, is a tributary of the Xiangjiang River which has a drainage area of 10 305 km^2 and 35 rain gauges. The area presents a complex topography, with elevations that range from 49 m to 2093 m, and features a humid subtropical monsoon climate with an average temperature of approximately 18.0℃ and a mean annual precipitation of approximately 1561 mm. The temporal and spatial distribution of precipitation within Mishui Basin is also uneven because of the atmospheric circulation and the annual precipitation that occurs mostly between April and September. During these months, particularly in June, basin-wide heavy rains occur continuously, thereby resulting in floods.

2.2 Data and processing

2.2.1 Satellite precipitation data

Satellite precipitation products used in this study are the

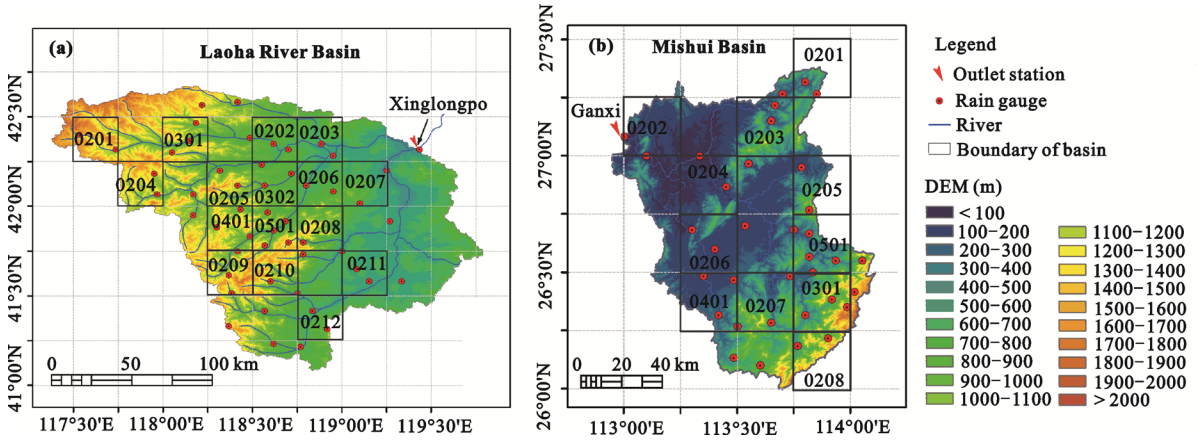

Fig. 1 Location of two study basins and distribution of rain gauge stations: (a) Laoha River Basin; (b) Mishui Basin. Also shown are the sampling strategies used in this study. Black squares indicate 16 selected 0.25° × 0.25° grid boxes in Laoha River Basin and 11 selected 0.25° × 0.25° grid boxes in Mishui Basin for verification of TMPA and CMORPH satellite precipitation products. Numbers are grid IDs, e.g., 0301 represents the first grid box that contains three rain gauge stations. TMPA means the Tropical Rainfall Measuring Mission (TRMM) Multi-satellite Precipitation Analysis, and CMORPH stands for Climate Prediction Center (CPC) morphing technique product

latest TMPA Version 7 and CMORPH Version 1.0 real-time and gauge-adjusted satellite precipitation products, i.e. T-rt, C-rt, T-adj and C-adj. The TMPA method retrieves T-rt through three consecutive stages: 1) polar-orbiting MW precipitation estimates are calibrated by TRMM MW estimates and then combined; 2) geostationary IR precipitation estimates are calibrated using the merged MW precipitation to fill in gaps of the MW coverage, and 3) MW and IR data are combined to form the real-time pure satellite precipitation product. In addition, the T-adj estimate adjusts the bias based on monthly rain gauge observations (Huffman *et al*., 2007). The CMORPH technique uses the directness of MW observations with cloud motion derived from IR data to estimate precipitation (Joyce *et al*., 2004). Currently, CMORPH products offer the following two high-resolution versions: one version shows temporal and spatial resolutions of 3 h and 0.25°, respectively, and the other version offers higher temporal and spatial resolutions of 30 min and 8 km, respectively, with both data covering the area from 60°S to 60°N globally. In the present research, we used the former CMORPH data, which is released as an official version. The resolution of the satellite precipitation products used in this study is 0.25° and 3 h. Three-hourly satellite precipitation products were aggregated to produce the accumulated daily and monthly precipitation for precision evaluation.

2.2.2 Gauged precipitation data

The observed daily precipitation data from 2000 to 2011 were derived from 52 rain gauge stations in Laoha River Basin and 35 rain gauge stations in Mishui Basin, that is, roughly two rain gauges within one 0.25° grid. Inverse Distance Weighting (IDW) was used to obtain the spatially distributed precipitation database of Laoha River Basin and Mishui Basin (Bartier and Keller, 1996). Basin topography data sets were obtained from the U.S. Geological Survey 30 arc-second global digital elevation model data.

2.3 Methods

2.3.1 Evaluation statistics

The validation statistical indices of Correlation Coefficient (CC), Mean Error (ME), Root Mean Square Error (RMSE), Relative Bias (BIAS), and Relative Absolute Bias (ABIAS) were employed to qualitatively evaluate the latest TMPA and CMORPH satellite precipitation data with rain gauge observations. CC shows the agreement between satellite precipitation and rain gauge observations. ME demonstrates the average difference between satellite precipitation and rain gauge observations. RMSE measures the absolute average error magnitude, and it assigns a greater weight to the larger errors. BIAS describes the systematic bias of satellite precipitation, whereas ABIAS represents the absolute bias of satellite precipitation. The formulas for CC, ME,

RMSE, BIAS, and ABIAS are given by:

$$CC = \frac{\sum_{i=1}^{n}(G_i - \bar{G})(S_i - \bar{S})}{\sqrt{\sum_{i=1}^{n}(G_i - \bar{G})^2}\sqrt{\sum_{i=1}^{n}(S_i - \bar{S})^2}} \quad (1)$$

$$ME = \frac{1}{n}\sum_{i=1}^{n}(S_i - G_i) \quad (2)$$

$$RMSE = \sqrt{\frac{1}{n}\sum_{i=1}^{n}(S_i - G_i)^2} \quad (3)$$

$$BIAS = \frac{\sum_{i=1}^{n}(S_i - G_i)}{\sum_{i=1}^{n}G_i} \times 100\% \quad (4)$$

$$ABIAS = \frac{\sum_{i=1}^{n}|S_i - G_i|}{\sum_{i=1}^{n}G_i} \times 100\% \quad (5)$$

where n is the total amount of rain gauge or satellite precipitation data; S_i and G_i are the ith values of the satellite precipitation data and rain gauge observations, respectively; and $\bar{S}$ and $\bar{G}$ are the mean values of the satellite precipitation data and rain gauge observations, respectively.

In addition, three categorical statistical indices, namely, Probability of Detection (POD), False-alarm Rate (FAR), and Critical Success Index (CSI), were adopted to measure the correspondence between satellite precipitation products and rain gauge observations. POD, which is also known as the hit rate, represents how often rain occurrences are detected correctly by the satellite. FAR denotes the fraction of cases in which the satellite records precipitation when rain gauges do not. CSI shows the overall fraction of precipitation events that are diagnosed correctly by the satellite. Rain or no-rain events are defined by the value of the threshold, and a precipitation threshold of 1.0 mm was used in this study. The perfect values of POD, FAR, and CSI were 1, 0, and 1, respectively. The formulas are given by:

$$POD = \frac{t_H}{t_H + t_M} \quad (6)$$

$$FAR = \frac{t_F}{t_H + t_F} \quad (7)$$

$$CSI = \frac{t_H}{t_H + t_M + t_F} \quad (8)$$

where H, M and F are different cases: H is observed rain that is correctly detected; M is observed rain that is not detected; F is detected but not observed rain; and t_H, t_M and t_F are the times of occurrence of the corresponding case. The details of these parameters refer to Ebert *et al*. (2007).

2.3.2 Evaluation methods

For comprehensive evaluation of the precision of four satellite precipitation products, we compared satellite estimates with rain gauge observations at different temporal (daily, monthly and yearly) and spatial (grid and basin) scales. Grid-based and basin-wide comparisons are two different spatial evaluation schemes. For grid-based evaluation, we selected grid boxes that contained a minimum of two gauges to reduce the scale errors caused by the direct comparison between gridded satellite estimates and the point-scale gauge data. Then, we used the mean value of all gauges inside each grid box as the ground truth for evaluation. This approach was adopted by numerous previous studies (Adler *et al*., 2003; Xue *et al*., 2013; Yong *et al*., 2014). Following this sampling strategy, 16 grid boxes of 0.25° × 0.25° that correspond to TMPA and CMORPH pixel resolution were selected for Laoha River Basin, while 11 grid boxes were adopted for Mishui Basin (Fig. 1). For basin-wide evaluation, we used the mean value of all grid boxes located in the basin for comparison. The benchmark precipitation data of the grid-based evaluation are supposed to be considerably more exact than that of the basin-wide evaluation. Meanwhile, basin-wide evaluation can better reflect the performance of the entire basin. In addition, the two spatial evaluation results can verify each other. Therefore, in this study, data from four satellite precipitation products of almost 12 years were roundly compared at multi-temporal and spatial scales in the high-latitude, semiarid Laoha River Basin and low-latitude, humid Mishui Basin.

3 Results and Discussion

3.1 Grid-based evaluation

Plots of daily and monthly estimates of T-rt, C-rt, T-adj,

and C-adj versus gauge observations for the 16 selected grid boxes in Laoha River Basin and 11 grid boxes in Mishui Basin are shown in Figs. 2 and 3, respectively. Figure 4 shows the temporal variations of average monthly precipitation for the selected grid boxes over the two selected basins. Table 1 provides the statistics of the daily and monthly performances at the selected grid boxes over these two basins. As shown in the figures and the statistical indices in the table, all the latest TMPA and CMORPH precipitation products evidently overestimate precipitation in the high-latitude Laoha River Basin and underestimate precipitation in the low-latitude Mishui Basin. For Laoha River Basin, both gauge-adjusted satellite precipitation products (i.e., T-adj and C-adj) are comprehensively better than the corresponding real-time satellite precipitation products (i.e., T-rt and C-rt). In particular, T-rt shows a serious overestimation (with a BIAS of 73.26%) of precipitation relative to the other three satellite precipitation products (Table 1, Figs. 2a–2d). In the comparison of the two real-time satellite precipitation estimates, C-rt offers an overall advantage over T-rt. For example, the daily CC, ME, BIAS, FAR, and CSI values are 0.60, 0.14 mm, 18.07%, 0.40, and 0.47 for C-rt and 0.55, 0.76 mm, 73.26%, 0.55, and 0.37 for T-rt, respectively (Table 1, Figs. 2a and 2b). Then, in the comparison of the two gauge-adjusted satellite precipitation estimates, C-adj also presents a slight advantage over T-adj; for example, the daily CC, ME, BIAS, FAR, and CSI values are 0.63, 0.03 mm, 8.10%, 0.39, and 0.47 for C-adj and 0.59, 0.07 mm, 11.72%, 0.46, and 0.41 for T-adj, respectively (Table 1, Figs. 2c and 2d).

By comparing values with those in the Laoha River Basin, these four sets TMPA and CMORPH estimates exhibit better CC values and lower BIAS (except C-rt) in the low-latitude Mishui basin. The precision of T-rt is considerably better than that in Laoha River Basin and is comparable with T-adj in the low-latitude Mishui Basin. A comparison between the two real-time satellite precipitation estimates indicates that T-rt exhibits an overall advantage over C-rt; for example, the daily ME, BIAS, POD, and CSI values are –0.29 mm, –6.60%, 0.63, and 0.52 for T-rt and –2.15 mm, –48.62%, 0.54, and 0.49 for C-rt, respectively (Table 1, Figs. 2e and 2f). Evidently, the performance of T-rt and C-rt in Mishui Basin is contrast with that in Laoha River Basin. In the comparison between the two gauge-adjusted satellite precipitation estimates, the T-adj offers a slight advantage over the C-adj for the large BIAS (–14.38%) of C-adj (Table 1, Figs. 2g and 2h).

Similar to the daily results, the monthly C-rt demonstrates an overall advantage over T-rt in Laoha River Basin but exhibits poorer performance than T-rt in Mishui Basin (Table 1, Figs. 3a, 3b, 3e and 3f). The monthly C-adj demonstrates comparable performance with T-adj in Laoha River Basin but poorer performance than T-adj in Mishui Basin (Table 1, Figs. 3c, 3d, 3g and 3h). In general, the gauge-adjusted products of TMPA and CMORPH largely outperformed real-time estimates at both daily and monthly time scales, thereby suggesting that the month-to-month gauge adjustments applied to the TMPA and CMORPH system improved the data accuracy of retrievals substantially (Table 1, Fig. 4). A comparison among the daily ME, RMSE, BIAS, and ABIAS values of gauge-adjusted products indicates that the month-to-month gauge adjustments render ME and BIAS close to 0, while the RMSE and ABIAS remain large. Therefore, the distribution of gauge-adjusted products at daily or sub-daily time scale still needs to be improved, and the robust near-real-time bias adjustment method needs to be investigated.

3.2 Basin-wide evaluation

In this section, to further determine the basin-wide precision of the satellite precipitation products, we first compared the satellite precipitation estimates with observations over the entire basin. The statistics of daily and monthly performances at the basin average scale are summarized in Table 2. Overall, as we expected, statistics with the basin-averaged data (except the ME and BIAS values) are better than the results obtained from grid-based comparisons in the previous section. Similar to the former grid scale research, the basin scale evaluation also demonstrates that the real-time CMORPH product in the high-latitude Laoha River Basin shows comparable precision with the two gauge-adjusted satellite precipitation estimations. By contrast, in the low-latitude Mishui Basin, the real-time TMPA product offers comparable precision with the two gauge-adjusted satellite precipitation products.

To further investigate the spatial error characteristics of four satellite precipitation products, we employed two spatial interpolation techniques to generate continuous precipitation surfaces over both validation basins. First,

the 0.25° × 0.25° gridded TMPA and CMORPH estimates were interpolated to 0.0625° × 0.0625° datasets using a simple cropping approach (Hossain and Huffman, 2008). Then, gauge observations were interpolated into the same resolution by IDW interpolation method. Subsequently, we computed three representative indices, CC, BIAS, and POD, to evaluate spatial rainfall patterns over the study basins. Figures 5 and 6 show the spatial distributions of CC, BIAS, and POD, which were computed from the interpolated daily precipitation datasets of the latest TMPA and CMORPH products against gauge observations at the 0.0625° × 0.0625° resolution grid. For Laoha River Basin, all four satellite precipitation products demonstrate similar distribution in their relative spatial performance. The poorest CC, BIAS, and POD values appear in the northwest (high elevation and latitude) and improve toward the southeast (low elevation and latitude) (Fig. 5). Except for POD, the CC and BIAS values of C-rt, T-adj, and C-adj are significantly better than that of T-rt, thereby indicating that the T-rt exhibits the poorest performance over the Laoha River Basin. The T-rt presents an apparent overestimation problem over the entire basin (Fig. 5e), and gauge-based adjustment in the researched product T-adj effectively minimized the systematic bias (Fig. 5g). Interestingly, the C-rt shows a small BIAS over the entire Laoha River Basin area, and the values of CC and POD are also comparable with the two gauge-adjusted satellite precipitation products. Thus, we can confidently use the C-rt in hydrologic process simulation and drought/flood disaster prediction over the high-latitude Laoha River Basin.

In Mishui Basin, the four satellite precipitation products show higher CC values and smaller BIAS (except the C-rt estimate) values than those of the Laoha River Basin, whereas the POD values are worse than those of Laoha River Basin (Figs. 5 and 6). In general, the satellite precipitation products (except the C-rt estimate) present better precisions in Mishui Basin than in Laoha River Basin. Moreover, T-rt shows a small BIAS value and high CC and POD values over the entire Mishui Basin, and the precision performance is comparable with the two gauge-adjusted satellite precipitation products. By contrast, C-rt, which exhibits good performance in the high-latitude Laoha River Basin, considerably underestimates precipitation over the low-latitude Mishui Basin and demonstrates poor precipitation retrieval performance. The error characteristics in the low-latitude Mishui Basin have a uniform spatial distribution. Moreover, spatial distribution does not display an apparent geo-topographic dependence, such as the case in the high-latitude Laoha River Basin.

3.3 Seasonal and inter-annual variability

To further confirm the stability of four satellite precipitation estimates at seasonal and inter-annual time scales, we investigated the seasonal and inter-annual variation of T-rt, C-rt, T-adj, and C-adj over both selected basins. Figure 7 shows the seasonal comparisons (CC, BIAS, and POD), including spring (March–May), summer (June–August), autumn (September–November), and winter (December–February) by computing at a daily time scale. In general, the gauge-adjusted products of TMPA and CMORPH obviously exhibit better performance than real-time products of TMPA and CMORPH over both basins and four seasons (Fig. 7). For the two real-time satellite precipitation products, T-rt seriously overestimated the gauge precipitation during all seasons, especially for winter, over the high-latitude Laoha River Basin, and C-rt fitted gauge precipitation well except with a slight underestimation in winter (Fig. 7c). Meanwhile, over the low-latitude Mishui Basin, C-rt seriously underestimated gauge precipitation during all seasons, and T-rt fitted gauge precipitation well except for a slight underestimation in winter (Fig. 7d). In addition, four satellite products show almost the worst CC and POD values in winter than those of the other three seasons over both basins (Figs. 7a, 7b, 7e and 7f). Accurate detection and estimation of precipitation during the winter months, especially for the high-latitude Laoha River Basin, remain a challenge for current satellite precipitation retrievals.

Figure 8 shows the yearly time series of precipitation, ME and BIAS of all selected grids for the latest TMPA and CMORPH satellite precipitation products against rain gauge observations during the period of Mar. 2000 to Dec. 2011. Over both selected basins, the gauge- adjusted products of TMAP and CMORPH present better agreement with gauge observations than real-time products of TMAP and CMORPH (Fig. 8). Results of the two real-time satellite precipitations are similar to those of the former analysis. Over the high-latitude Laoha River Basin, T-rt seriously overestimated gauge precipitation in all years, and C-rt fitted the gauge

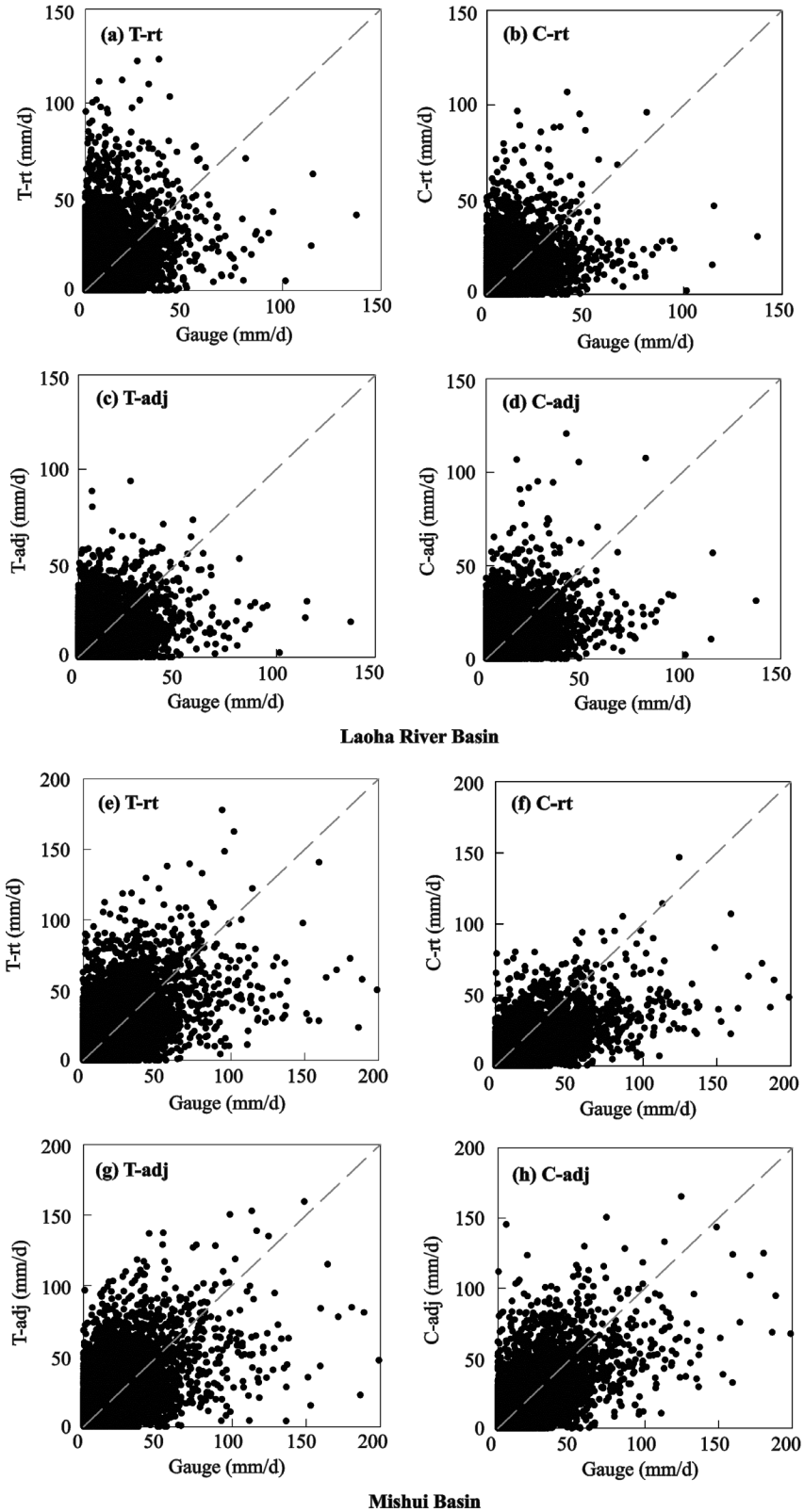

Fig. 2 Scatterplots of grid-based daily precipitation comparison between satellite estimates and rain gauge observations at 16 selected grid boxes in Laoha River Basin (a–d) and 11 selected grid boxes in Mishui Basin (e–h), respectively. T-rt is Version-7 real-time TMPA, C-rt means Version-1.0 real-time CMORPH, T-adj stands Version-7 gauge-adjusted TMPA, and C-adj is Version-1.0 gauge-adjusted CMORPH

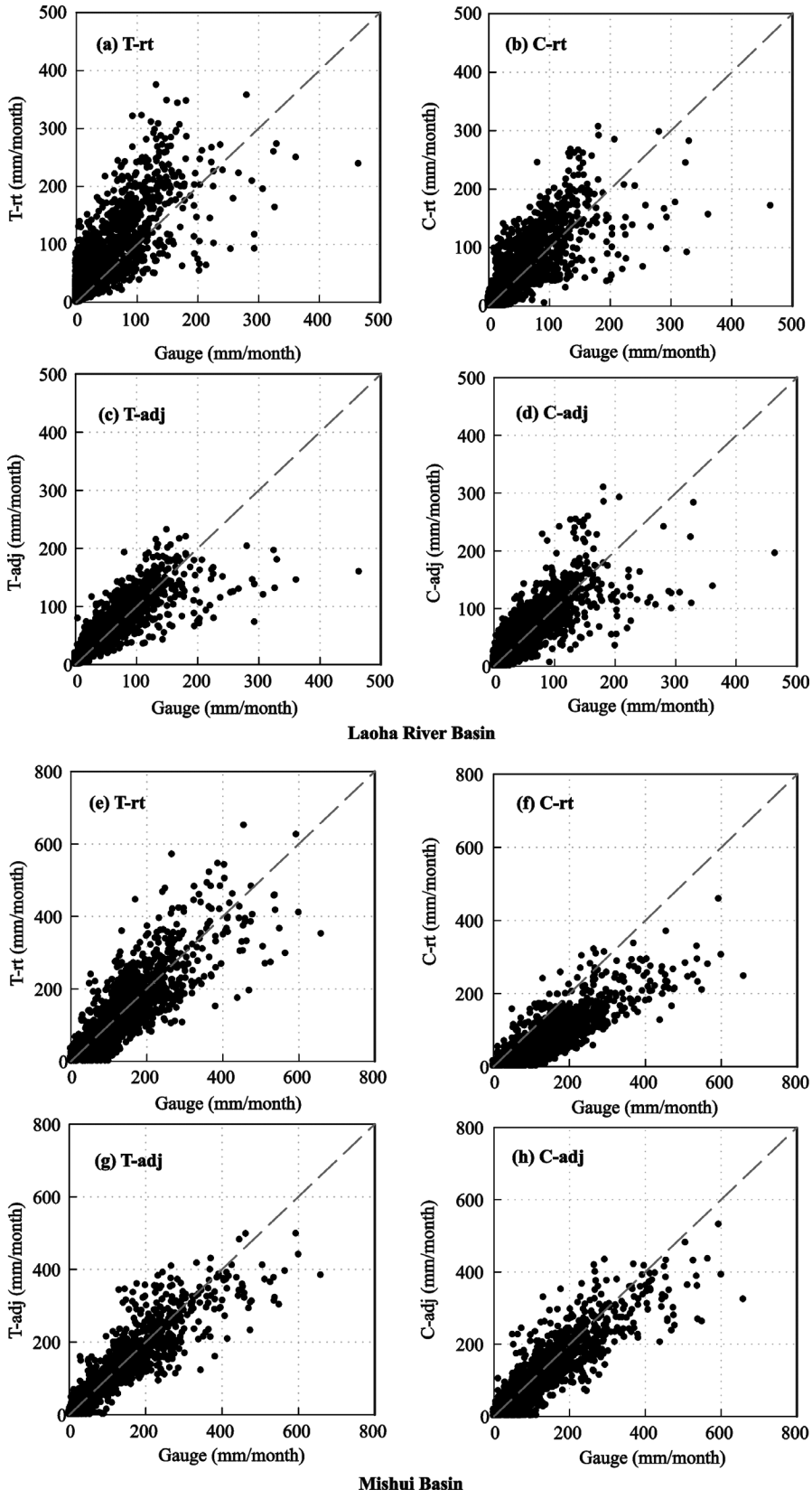

Fig. 3 Scatterplots of grid-based monthly precipitation comparison between satellite estimates and rain gauge observations at 16 selected grid boxes in Laoha River Basin (a–d) and 11 selected grid boxes in Mishui Basin (e–h), respectively

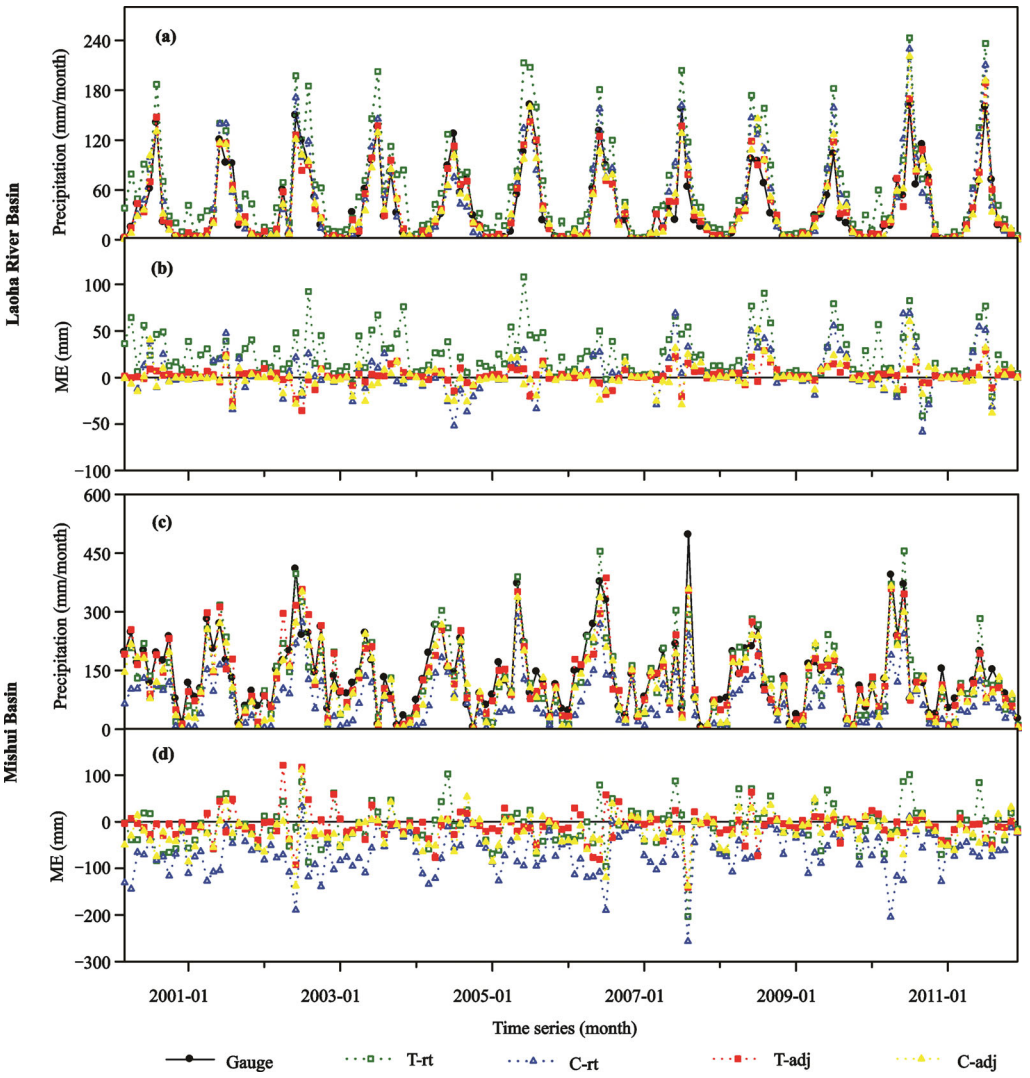

Fig. 4 Temporal series of mean monthly precipitation of 16 selected grid boxes in Laoha River Basin and that of 11 selected grid boxes in Mishui Basin, respectively: (a and c) monthly precipitation time series, and (b and d) ME. ME means Mean Error

Table 1 Statistical measures of grid-based comparison of latest TMPA and CMORPH precipitation estimates at daily and monthly time scales in high-latitude Laoha River Basin and low-latitude Mishui Basin, respectively

Time scale	Statistical index	Laoha River Basin				Mishui Basin			
		T-rt	C-rt	T-adj	C-adj	T-rt	C-rt	T-adj	C-adj
Daily	CC	0.55	0.60	0.59	0.63	0.69	0.72	0.68	0.74
	ME (mm)	0.76	0.14	0.07	0.03	–0.29	–2.15	–0.26	–0.65
	RMSE (mm)	5.43	4.14	4.02	3.86	8.70	8.04	8.84	7.83
	BIAS (%)	73.26	18.07	11.72	8.10	–6.60	–48.62	–5.64	–14.38
	ABIAS (%)	153.78	108.72	109.00	100.35	79.80	71.60	82.11	71.90
	POD	0.71	0.68	0.63	0.67	0.63	0.54	0.61	0.62
	FAR	0.55	0.40	0.46	0.39	0.25	0.17	0.23	0.19
	CSI	0.37	0.47	0.41	0.47	0.52	0.49	0.52	0.54
Monthly	CC	0.85	0.87	0.93	0.90	0.84	0.85	0.89	0.88
	ME (mm)	23.14	4.11	2.09	0.82	–8.92	–65.30	–8.04	–19.87
	RMSE (mm)	43.68	29.68	20.10	24.20	59.13	85.69	47.40	53.02
	BIAS (%)	73.26	18.07	11.72	8.10	–6.60	–48.62	–5.64	–14.38
	ABIAS (%)	87.78	50.98	33.62	39.92	32.52	50.95	23.97	28.84

Notes: TMPA means the Tropical Rainfall Measuring Mission (TRMM) Multi-satellite Precipitation Analysis, and CMORPH stands for Climate Prediction Center (CPC) morphing technique product. T-rt is Version-7 real-time TMPA, C-rt means Version-1.0 real-time CMORPH, T-adj stands for Version-7 gauge-adjusted TMPA, and C-adj is Version-1.0 gauge-adjusted CMORPH. CC is Correlation Coefficient, ME stands for Mean Error, RMSE means Root Mean Square Error, BIAS is Relative Bias, ABIAS means Relative Absolute Bias, POD is Probability of Detection, FAR means False-alarm Rate, and CSI stands for Critical Success Index

Table 2 Statistical measures of basin-wide comparison of latest TMPA and CMORPH precipitation estimates at daily and monthly time scales in high-latitude Laoha River Basin and low-latitude Mishui Basin, respectively

Time scale	Statistical index	Laoha River Basin				Mishui Basin			
		T-rt	C-rt	T-adj	C-adj	T-rt	C-rt	T-adj	C-adj
Daily	CC	0.71	0.72	0.77	0.77	0.78	0.79	0.78	0.81
	ME (mm)	0.85	0.24	0.18	0.13	–0.30	–2.10	–0.21	–0.57
	RMSE (mm)	3.49	2.79	2.30	2.44	6.21	6.41	6.29	5.73
	BIAS (%)	79.64	22.82	16.62	12.14	–6.97	–48.60	–4.84	–13.30
	ABIAS (%)	123.35	87.44	79.63	77.93	61.79	62.91	62.57	58.51
	POD	0.86	0.80	0.80	0.78	0.73	0.58	0.73	0.68
	FAR	0.48	0.29	0.34	0.27	0.16	0.07	0.15	0.12
	CSI	0.48	0.60	0.56	0.60	0.65	0.55	0.65	0.62
Monthly	CC	0.91	0.92	0.98	0.95	0.89	0.88	0.94	0.92
	ME (mm)	26.01	7.45	5.43	3.96	–9.15	–63.84	–6.36	–17.47
	RMSE (mm)	37.18	22.53	10.70	13.92	45.65	79.94	33.06	39.41
	BIAS (%)	79.64	22.82	16.62	12.14	–6.97	–48.60	–4.84	–13.30
	ABIAS (%)	84.22	43.57	21.82	26.67	26.31	49.38	16.60	22.29

Note: meanings of all the abbreviations see Table 1

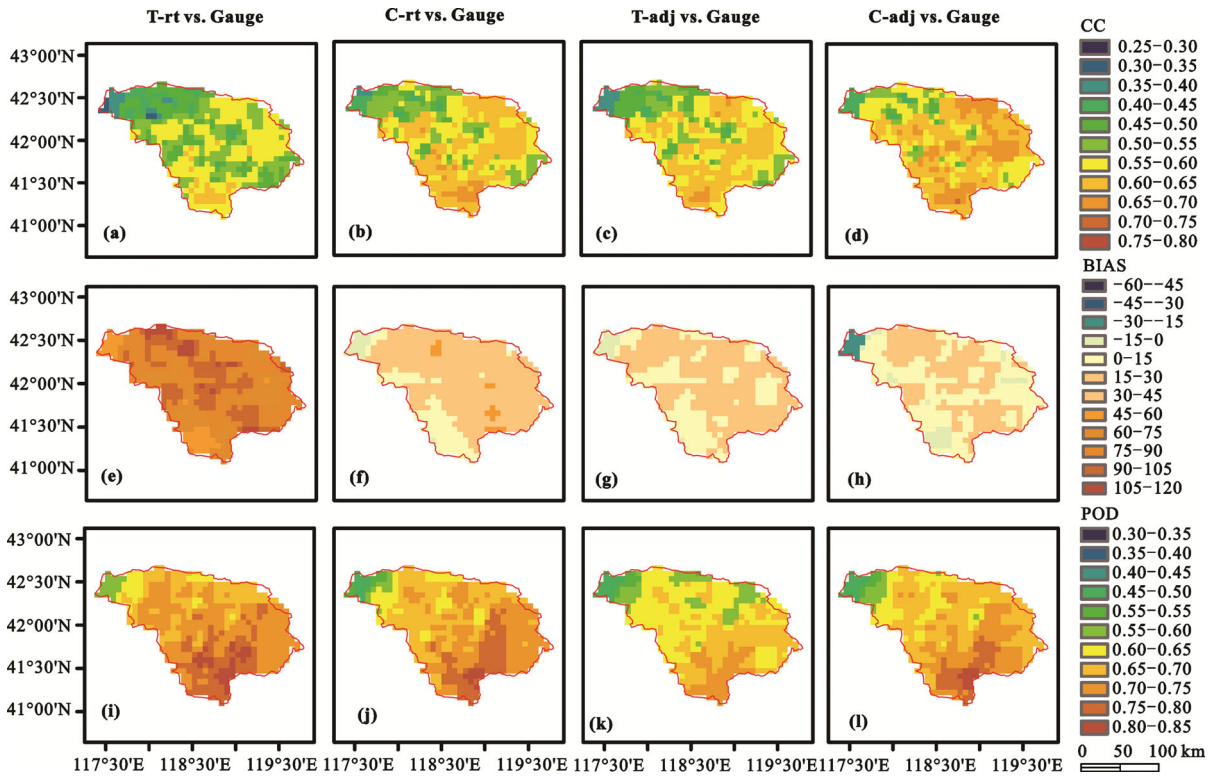

Fig. 5 Spatial distributions of statistical indices computed from T-rt (1st column), C-rt (2nd column), T-adj (3rd column), and C-adj (4th column) daily precipitation at 0.0625° × 0.062° resolution in Laoha River Basin: (a–d) CC, (e–h) BIAS, and (i–l) POD. CC is Correlation Coefficient, BIAS means Relative Bias, and POD stands for Probability of Detection

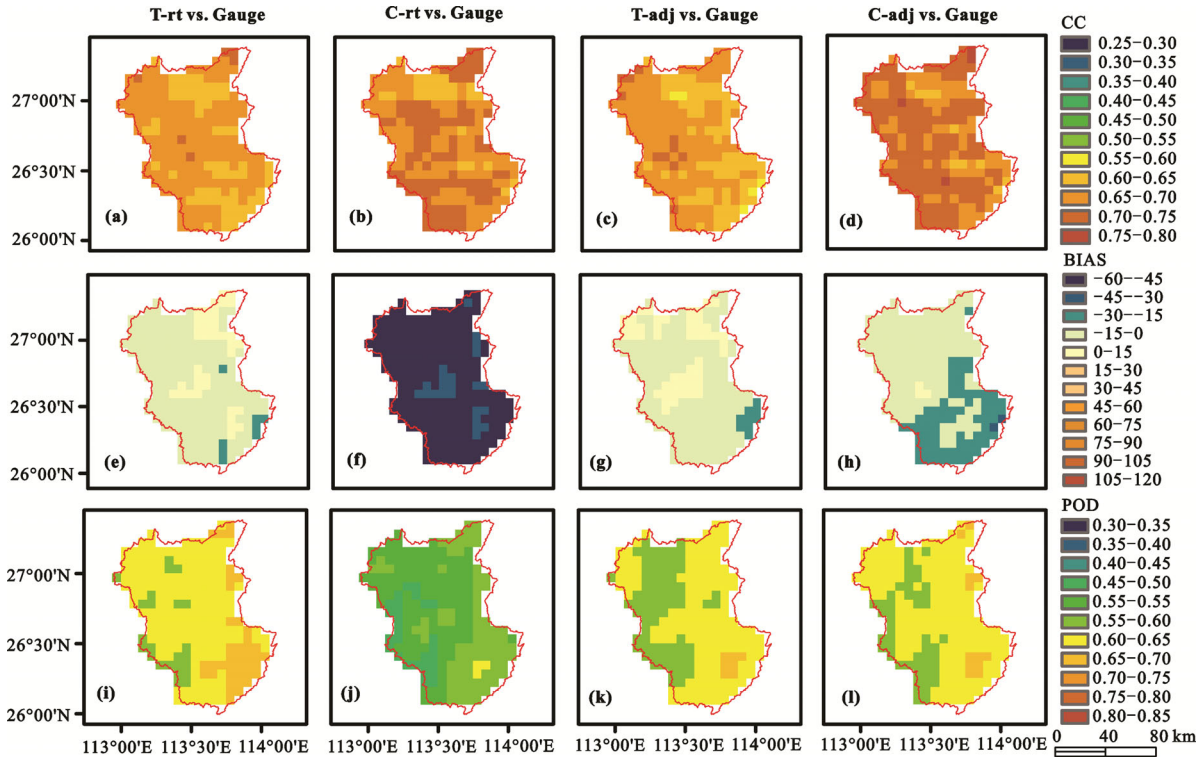

Fig. 6 Spatial distributions of statistical indices computed from T-rt (1st column), C-rt (2nd column), T-adj (3rd column), and C-adj (4th column) daily precipitation at 0.0625° × 0.062° resolution in Mishui Basin: (a–d) CC, (e–h) BIAS, and (i–l) POD. CC is Correlation Coefficient, BIAS means Relative Bias, and POD stands for Probability of Detection

precipitation well except for underestimation in 2004 and overestimation in 2007 to 2009 (Figs. 8a, 8c and 8e). Meanwhile, over the low-latitude Mishui Basin, C-rt seriously underestimated gauge precipitation in all years, and T-rt fitted the gauge precipitation well with comparable precision with two gauge-adjusted satellite precipitation products (Figs. 8b, 8d and 8f). By comparing the BIAS over the two basins, we concluded that the precisions of the four satellite precipitation products present large inter-annual variability over the high-latitude Laoha River Basin, whereas the yearly precisions are relatively stable over the low-latitude Mishui Basin (Figs. 8e and 8f).

3.4 Error characteristic analysis and discussion

Numerous previous studies have pointed out that the errors of satellite precipitation estimates show evident dependency on the precipitation retrieval algorithm, the nature of sensor that was used, surface condition (ocean or land), and precipitation type among others (Pan *et al*., 2010; Gebregiorgis and Hossain, 2015). Following research on the dependence of error on seasonality in the previous section, we will analyze rain rate dependency and discuss the climate condition dependency of the error characteristic for the four satellite precipitation products over the two selected basins in this section.

Figure 9 shows the intensity distributions of daily precipitation amounts and daily number of precipitation events for the selected grid boxes in Laoha River Basin and Mishui Basin, respectively. The intensity distributions of daily precipitation amount are computed as a ratio of the sum of precipitation rates in each bin to the total sum of gauge precipitation rates. Similarly, the intensity distributions of daily precipitation events are computed as a ratio between the sum of precipitation days in each bin and the total days. In this section, only the grid precipitation that is equal to or greater than 1 mm can be selected to compute intensity distributions. T-rt overestimated both the precipitation amount and event in all bins over Laoha River Basin, whereas the performance approached a similar level of quality as research precipitation products over Mishui Basin. By contrast, C-rt performs well over Laoha River Basin, whereas the product exhibits series underestimation over Mishui Basin. Notably, all satellite precipitation products obviously overestimate precipitation at light

rain rates (< 8 mm/d) both at precipitation amounts and events in Laoha River Basin but underestimate the amount and events in Mishui Basin. In addition, the results demonstrate that all satellite precipitation products underestimate precipitation amounts at high rain rates (> 128 mm/d) in Mishui Basin (Fig. 9b).

For the climate condition, the high-latitude Laoha River Basin is a temperate semiarid continental monsoon type location with a mean annual precipitation of 424 mm. By contrast, the low-latitude Mishui Basin is a humid subtropical monsoon type location with a mean annual precipitation of 1561 mm. Climate type is another influential factor of satellite precipitation retrieval errors. All four satellite precipitation products overestimated precipitation in the semiarid Laoha River Basin but underestimated precipitation in the humid Mishui Basin. This underestimation is particularly evident for the two real-time satellite precipitation products. Except for C-rt, the precisions of the other three satellite precipitation products in the humid Mishui Basin comprehensively outperform those in the semiarid Laoha River Basin. These findings are consistent with the results of Shen *et al*. (2010) and Qin *et al*. (2014), thereby demonstrating that the satellite products vary for different regions and different precipitation regimes, with better comparison statistics observed over wet regions in China. In addition, the C-rt underestimates precipitation and T-rt overestimates precipitation in China. C-rt reaches similar accuracy levels with gauge-adjusted satellite precipitation products in the high-latitude semiarid Laoha River Basin. This finding is important and significant to obtain the best hydrometeorological applications of multiple real-time satellite precipitation products in

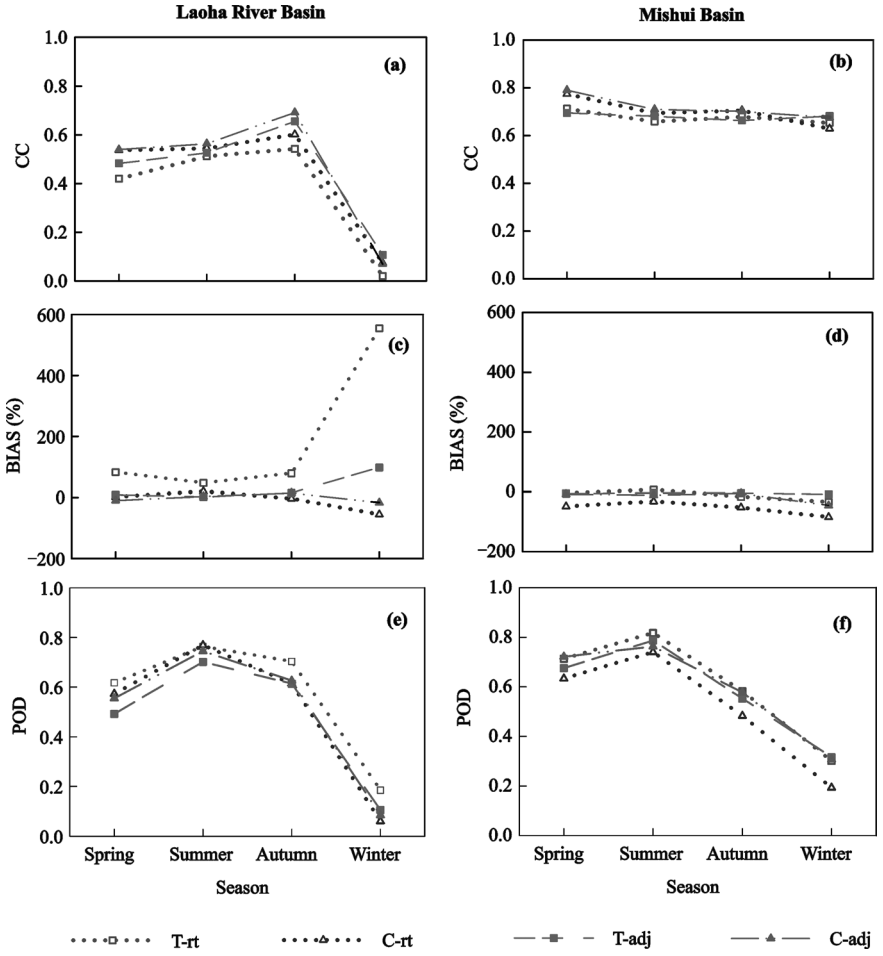

Fig. 7 Grid-based seasonal comparison of latest TMPA and CMORPH precipitation estimates at daily time scales in high-latitude Laoha River Basin and low-latitude Mishui Basin, respectively: (a, b) CC, (c, d) BIAS, and (e, f) POD. CC is Correlation Coefficient, BIAS means Relative Bias, and POD stands for Probability of Detection

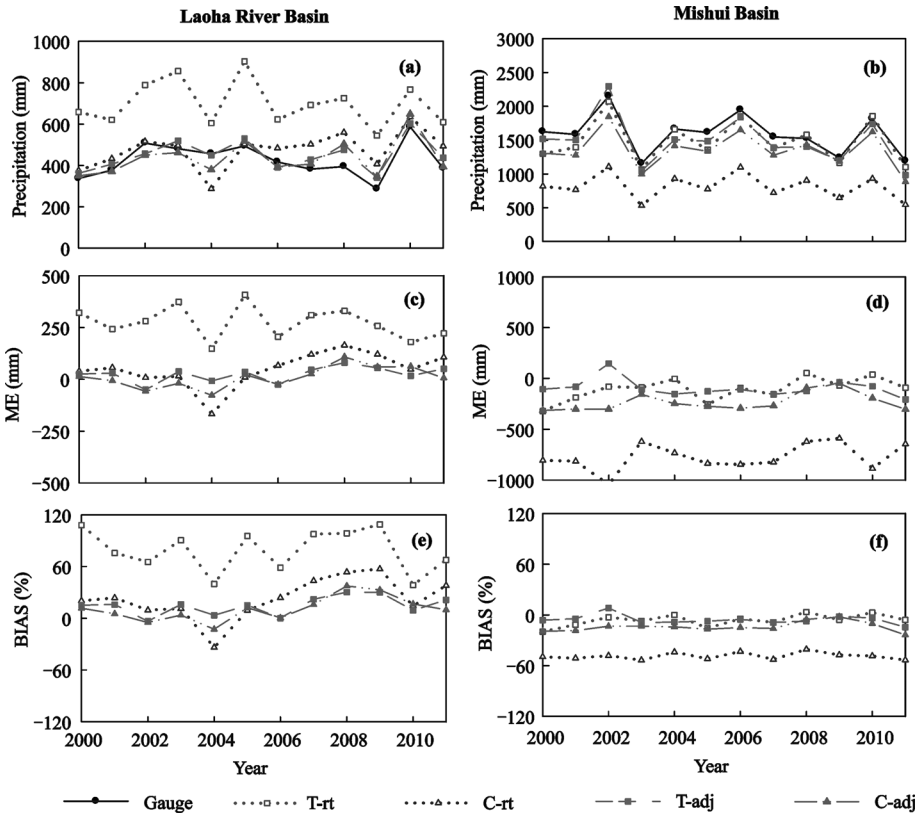

Fig. 8 Temporal series of average yearly precipitation of 16 selected grid boxes in Laoha River Basin and 11 selected grid boxes in Mishui Basin, respectively: (a, b) yearly precipitation series, (c, d) ME, and (e, f) BIAS. ME is Mean Error, BIAS means Relative Bias

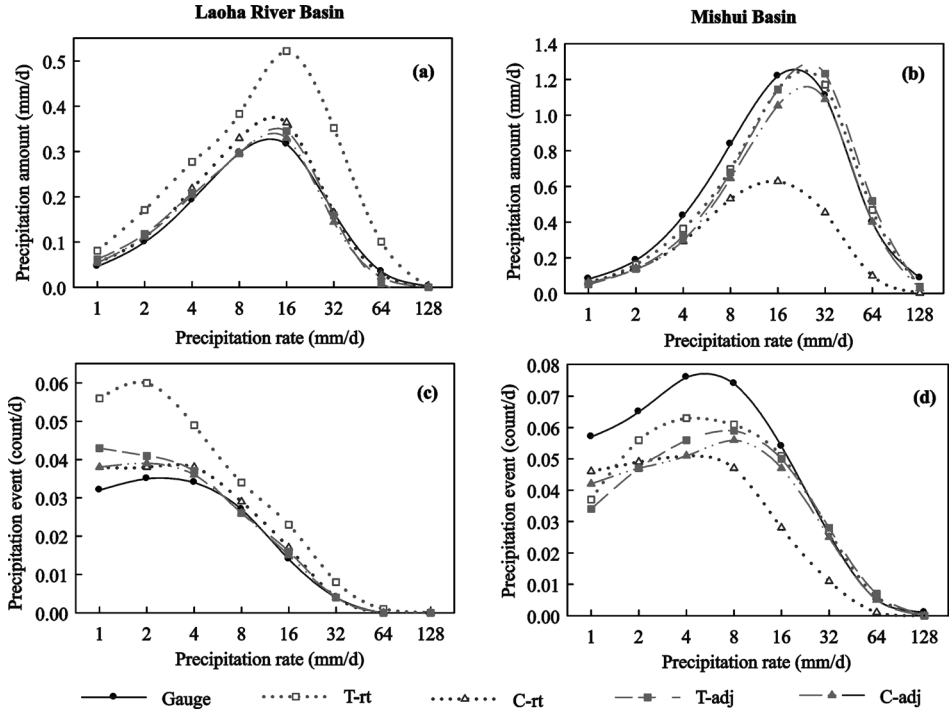

Fig. 9 Daily precipitation amount (a, b) and daily precipitation events (c, d) as a function of precipitation rate for 16 selected grid boxes in Laoha River Basin and 11 selected grid boxes in Mishui Basin, respectively

different Chinese regions using the respective advantages of each satellite precipitation data. In addition, for the two selected basins, the high-latitude Laoha River Basin is studied beyond the TRMM TMI/PR nominal coverage (38°N–38°S), and the low-latitude Mishui Basin is studied in the TRMM TMI/PR nominal coverage. This coverage may affect the precision performance of TMPA and CMORPH satellite precipitation products in the two basins (Yong *et al*., 2014).

4 Conclusions

This study focuses on comprehensive evaluation of the latest TMPA Version 7 and CMORPH Version 1.0 satellite precipitation products with dense rain gauge observations at medium watershed scale. The precision and error characteristics of the latest real-time version T-rt and C-rt, as well as those of the gauge-adjusted version T-adj and C-adj, were evaluated at multiple temporal and spatial scales for a period of almost 12 years (Mar. 2000 to Dec. 2011) over the high-latitude semiarid Laoha River Basin and the low-latitude humid Mishui Basin in China, respectively. Several main conclusions are drawn as follows:

(1) TMPA and CMORPH products tend to overestimate precipitation over the high-latitude semiarid Laoha River Basin and underestimate the amount over the low-latitude humid Mishui Basin. Overall, the satellite precipitation products exhibit better performance over Mishui Basin than over Laoha River Basin. In a comprehensive analysis of the daily and monthly statistical indices, the gauge-adjusted product of C-adj exhibits the best performance over Laoha River Basin, and the T-adj shows the best performance over Mishui Basin. The two gauge-adjusted products demonstrate high effectiveness in water resource management.

(2) Accuracies of the two real-time satellite precipitation products demonstrate large variability in the two validation basins. C-rt reaches similar accuracy levels with the two satellite precipitation products in the Laoha River Basin, and T-rt performs well in the Mishui Basin. This finding is important and significant for hydrometeorological applications of the two real-time satellite precipitation products for other similar latitudes and climate conditions in Chinese regions.

(3) For the seasonal and inter-annual time scales, the gauge-adjusted products show better agreement with gauge observations than real-time products over both basins. The four satellite precipitations exhibit poor performance in winter than in the other three seasons. We argue that accurate detection and estimation of precipitation during the winter months, especially for high-latitude regions, remain a challenge for current satellite precipitation retrievals. Four satellite precipitation products present large inter-annual variabilities over the Laoha River Basin, while annual precisions are relatively stable over the Mishui Basin.

(4) The intensity distributions of daily precipitation demonstrates that all satellite precipitation products obviously overestimate light rain rate (< 8 mm/d) both at precipitation amounts and events in Laoha River Basin but underestimate in Mishui Basin. Moreover, all the satellite precipitation products underestimate precipitation amounts at high rain rate (> 128 mm/d) in Mishui Basin.

This implemented analysis provides detailed information on the error characteristics associated with the latest TMPA and CMORPH precipitation products over two different latitudes and climate conditions in basins in China. The information will offer satellite precipitation users an improved understanding of the applicability of the latest TMPA and CMORPH products for water resource management, hydrologic process simulation, and hydrometeorological disaster prediction in similar Chinese regions. Moreover, the results will useful for IMERG algorithm development and update in the GPM-era.

References

Adler R F, Huffman G J, Chang G J *et al*., 2003. The version 2 Global Precipitation Climarology Project (GPCP) monthly precipitation analysis (1979–present). *Journal of Hydrometeorology*, 4(6): 1147–1167. doi: 10.1175/1525-7541(2003)004<1147:TVGPCP>2.0.CO;2

Bartier P M, Keller C P, 1996. Multivariate interpolation to incorporate thematic surface data using inverse distance weighting (IDW). *Computers & Geosciences*, 22(7): 795–799. doi: 10.1016/0098-3004(96)00021-0

Behrangi A, Khakbaz B, Jaw T C *et al*., 2011. Hydrologic evaluation of satellite precipitation products over a mid-size basin. *Journal of Hydrology*, 397(3–4): 225–237. doi: 10.1016/j.jhydrol.2010.11.043

Bitew M M, Gebremichael M, 2011. Evaluation of satellite rainfall products through hydrologic simulation in a full distributed hydrologic model. *Water Resources Research*, 47(6):

W06526. doi: 10.1029/2010WR009917

Chen S, Hong Y, Cao Q *et al*., 2013. Similarity and difference of the two successive V6 and V7 TRMM multisatellite precipitation analysis performance over China. *Journal of Geophysical Research*, 118(23): 13060–13074. doi: 10.1002/2013JD019964

Ebert E E, Janowiak J E, Kidd C, 2007. Comparison of near-real-time precipitation estimates from satellite observations and numerical models. *Bulletin of the American Meteorological Society*, 88(1): 47–64. doi: 10.1175/BAMS-88-1-47

Gebregiorgis A S, Hossain F, 2015. How well can we estimate error variance of satellite precipitation data around the world? *Atmospheric Research*, 154: 39–59. doi: 10.1016/j.atmosres.2014.11.005

Hong Y, Adler R F, Hossain F *et al*., 2007. A first approach to global runoff simulation using satellite rainfall estimation. *Water Resources Research*, 43(8): W08502. doi: 10.1029/2006WR005739

Hossain F, Huffman G J, 2008. Investigating error metrics for satellite rainfall at hydrologically relevant scales. *Journal of Hydrometeorology*, 9(3): 563–575. doi: 10.1175/2007JHM925.1

Hou A Y, Kakar R K, Neeck S *et al.*, 2014. The global precipitation measurement mission. *Bulletin of the American Meteorological Society*, 95(5): 701–722. doi: 10.1175/BAMS-D-13-00164.1

Hu Q F, Yang D W, Li Z *et al*., 2014. Multi-scale evaluation of six high-resolution satellite monthly rainfall estimates over a humid region in China with dense rain gauges. *International Journal of Remote Sensing,* 35(4): 1272–1294. doi: 10.1080/01431161.2013.876118

Huffman G J, Adler R F, Bolvin D T *et al*., 2007. The TRMM Multisatellite Precipitation Analysis (TMPA): quasi-global, multiyear, combined-sensor precipitation estimates at fine scales. *Journal of Hydrometeorology*, 8(1): 38–55. doi: 10.1175/JHM560.1

Huffman G J, Bolvin D T, 2013. Real-Time TRMM Multi- Satellite Precipitation Analysis data set documentation. ftp://meso-a.gsfc.nasa.gov/pub/trmmdocs/rt/3B4XRT_doc_V7.pdf

Jiang S H, Ren L L, Hong Y *et al*., 2012. Comprehensive evaluation of multi-satellite precipitation products with a dense rain gauge network and optimally merging their simulated hydrological flows using the Bayesian Model Averaging Method. *Journal of Hydrology*, 452–453: 213–225. doi: 10.1016/j. jhydrol.2012.05.055

Jiang S H, Ren L L, Hong Y *et al*., 2014. Improvement of multi-satellite real-time precipitation products for ensemble streamflow simulation in a middle latitude basin in South China. *Water Resources Management*, 28(8): 2259–2278. doi: 10.1007/s11269-014-0612-4

Jiang S H, Ren L L, Yong B *et al*., 2010. Evaluation of high-resolution satellite precipitation products with surface rain gauge observations from Laohahe Basin in northern China. *Water Science and Engineering,* 3(4): 405–417. doi: 10.3882/j.issn.1674-2370.2010.04.004

Joyce R J, Janowiak J E, Arkin P A *et al*., 2004. CMORPH: A method that produces global precipitation estimates from passive microwave and infrared data at high spatial and temporal resolution. *Journal of Hydrometeorology*, 5(3): 487–503. doi: org/10.1175/1525-7541

Kidd C, Huffman G, 2011. Global precipitation measurement. *Meteorological Applications*, 18(3): 334–353. doi: 10.1002/met.284

Kucera P A, Ebert E E, Turk F J *et al*., 2013. Precipitation from space: advancing Earth System Science. *Bulletin of the American Meteorological Society*, 94(3): 365–375. doi: org/10.1175/BAMS-D-11-00171.1

Li X H, Zhang Q, Xu C Y, 2014. Assessing the performance of satellite-based precipitation products and its dependence on topography over Poyang Lake Basin. *Theoretical and Applied Climatology*, 115(3): 713–729. doi: 10.1007/s00704-013-0917-x

Li Z, Yang D W, Hong Y, 2013. Multi-scale evaluation of high-resolution multi-sensor blended global precipitation products over the Yangtze River. *Journal of Hydrology*, 500: 157–169. doi: 10.1016/j.jhydrol.2013.07.023

Liu J Z, Duan Z, Jiang J C *et al*., 2014. Evaluation of three satellite precipitation products TRMM 3B42, CMORPH, and PERSIANN over a subtropical watershed in China. *Advance in Meteorology*, 151239. doi: org/10.1155/2015/151239

Pan M, Li H, Wood E, 2010. Assessing the skill of satellite based precipitation estimates in hydrologic applications. *Water Resources Research*, 46(9): W09535. doi: 10.1029/2009WR008290

Qin Y X, Chen Z Q, Shen Y *et al*., 2014. Evaluation of satellite rainfall estimates over the Chinese Mainland. *Remote Sensing*, 6(11): 11649–11672. doi: 10.3390/rs61111649

Shen Y, Xiong A Y, Wang Y *et al*., 2010. Performance of high-resolution satellite precipitation products over China. *Journal of Geophysical Research*, 115(D2): D02114. doi: 10.1029/2009JD012097

Shen Y, Zhao P, Pan Y *et al*., 2014. A high spatiotemporal gauge-satellite merged precipitation analysis over China. *Journal of Geophysical Research*, 119(6): 3063–3075. doi: 10. 1002/2013JD020686

Su F G, Hong Y, Lettenmaier D P *et al*., 2008. Evaluation of TRMM Multi-satellite Precipitation Analysis (TMPA) and its utility in hydrologic prediction in La Plata Basin. *Journal of Hydrometeorology*, 9(4): 622–640. doi: org/10.1175/2007JHM944.1

Tong K, Su F G, Yang D *et al*., 2014. Evaluation of satellite precipitation retrievals and their potential utilities in hydrologic modeling over the Tibetan Plateau. *Journal of Hydrology*, 519: 423–437. doi: 10.1016/j.jhydrol.2014.07.044

Wu H, Adler R F, Tian Y D *et al*., 2014. Real-time global flood estimation using satellite-based precipitation and a coupled land surface and routing model. *Water Resources Research*, 50(3): 2693–2717. doi: 10.1002/2013WR014710.

Xie P P, 2013. CMORPH_V1.0_README. ftp://ftp.cpc.ncep.noaa.gov/precip/CMORPH_V1.0

Xue X W, Hong Y, Limaye A S *et al*, 2013. Statistical and hydrological evaluation of TRMM-based Multi-satellite Precipita-

tion Analysis over the Wangchu Basin of Bhutan: are the latest satellite precipitation products 3B42V7 ready for use in ungauged basins? *Journal of Hydrology*, 499: 91–99. doi: 10.1016/j.jhydrol.2013.06.042

Yong B, Chen B, Gourley J J *et al*., 2014. Intercomparison of the Version-6 and Version-7 TMPA precipitation products over high and low latitudes basins with independent gauge networks: is the newer version better in both real-time and post-real-time analysis for water resources and hydrologic extremes? *Journal of Hydrology*, 508: 77–87. doi: 10.1016/j.jhydrol.2013.10.050

Yong B, Hong Y, Ren L L *et al*., 2012. Assessment of evolving TRMM-based multisatellite real-time precipitation estimation methods and their impacts on hydrologic prediction in a high latitude basin. *Journal of Geophysical Research*, 117(9): D09108. doi: 10.1029/2011JD017069